## REMARKS

New claims 20-22 are added herein. Support is found, for example, at the paragraph bridging pages 10 to 11 of the specification, the first full paragraph at page 13, Examples 1 and 2 in the specification as filed. No new matter is presented.

### Response to Claim Rejections under 35 U.S.C. § 103

**A.      Koji et al in view of Wells**

Claims 1, 4-6, 9-11 and 14-19 are rejected under 35 U.S.C. § 103(a) as allegedly being unpatentable over Koji et al (JP 07-304620) in view of Wells et al (US 4,356,280).

Applicants traverse the rejection and submit that the Examiner has not set forth a *prima facie* showing of obviousness.

The present invention relates to an antimicrobial composition comprising: (1) tetravalent metal phosphate-based antimicrobial particles represented by Formula (1); and (2) inorganic compound particles having a Mohs hardness of equal to or less than 6. The maximum particle size of these particles is substantially equal to or less than 10 μm. The tetravalent metal phosphate-based antimicrobial particles and the inorganic compound particles have an average particle size of 0.1 to 5μm, and the average particle size of the inorganic compound particles is equal to or smaller than the average particle size of the tetravalent metal phosphate-based antimicrobial particles.

As previously noted, Koji et al does not disclose, teach nor suggest the feature of the average particle size of the inorganic compound particles is equal to or smaller than the average particle size of the tetravalent metal phosphate-based antimicrobial particles as recited in present claim 1 for the reasons of record, which are incorporated herein.

In the Action dated March 19, 2009, the Examiner asserts that the calcium phosphate salt system and the zeolite system taught by Koji et al are comparison references and therefore one of ordinary skill in the art would formulate the tetravalent metal phosphate system (i.e., phosphoric acid zirconium salt system) having approximately the same particle size as the comparison references calcium phosphate salt system and zeolite system (i.e., 1.2 or 2.6 μm).

However, Applicants submit that Koji et al does not teach nor suggest anything about the average particle size of tetravalent metal phosphate-based antimicrobial particles. The calcium phosphate system of Koji et al does not correspond to the tetravalent metal phosphate-based particles of the present invention and there is no motivation for one of ordinary skill in the art to combine the references and to use the tetravalent metal phosphate-based antimicrobial particles together with the inorganic compound particles such as titanium dioxide.

As previously noted, Koji et al addresses the problem of discoloration and deterioration of the resin. On the other hand, the tetravalent metal phosphate-based particles of the present invention cause the problem that an area of equipment that is running in contact with a molding is easily worn when the molding is produced by adding the tetravalent metal phosphate-based antimicrobial agent to a resin (described at page 1, lines 20-23 of the present specification). When using a calcium phosphate salt system as in Koji et al, the above-mentioned problem in the present invention does not occur. Although Koji et al discloses the use of a calcium phosphate salt system having the average particle size of 1.2 μm, there is no apparent reason to use tetravalent metal phosphate particles having an average particle size of 0.1 to 5 μm as presently claimed. As stated above, the calcium phosphate system of Koji et al does not correspond to the tetravalent metal phosphate-based antimicrobial particles of the present invention. Therefore,

Koji et al does not teach nor suggest the use of the tetravalent metal phosphate-based particles within the claimed range.

Moreover, Koji et al does not describe the relation of the particle size between the tetravalent metal phosphate-based particles and the inorganic compound particles.

The Examiner relies on Wells as teaching that titanium dioxide is a particularly preferred additive in spinning highly viscous synthetic polymer fibers used to decrease the luster resulting fiber spun from the molten polymer, wherein the preferred average diameter is 0.1 to 0.5 μm, most preferably 0.2 μm or less. Thus, the Examiner asserts that one of ordinary skill in the art would have been motivated to use the titanium dioxide with an average diameter of approximately 0.2 μm, which would have been smaller than the particle size of the tetravalent metal phosphate-based particles.

Applicants disagree.

In column 3, lines 2 to 5, Wells it is describes that "Anatase titanium dioxide is the preferred form for delustering synthetic fibers because it is softer than rutile, thereby giving lower abrasiveness in yarn processing equipment". One skilled in the art would not be motivated to apply a powder material harder than the anatase titanium dioxide to the dispersion for incorporation with polyamide or polyester polymer. In other word, Wells **teaches away** from particles harder than the anatase titanium dioxide.

The tetravalent metal phosphate-based antimicrobial particles have a greater Mohs hardness than the inorganic compound particles used in the present invention. Applicants submit documents herewith that disclose that "NZP" has a Mohs hardness of more than 6.5. NZP means sodium-zirconium-phosphates and its crystal structural analogs, and NZP corresponds to the compound represented by formula (1) of the present invention, wherein a=O.

Document No. 1 (V. I. Pet'kov and E. A. Asabina, "Thermophysical properties of NZP ceramics (a review)", Glass and Ceramics, vol. 61, Nos. 7-8, 2004, pp. 233-239) discloses that NZP has Rockwell hardness of HRA 90 (page 234, left column, line 1).

Document No. 2 (Mineral Hardness Conversion Chart from CiDRA® Precision Services, LLC), HRA 86 is equivalent to a Mohs hardness of 6.5. Therefore, NZP has Mohs hardness of greater than 6.5 (HRA 90) and the hardness is like that of quartz.

The tetravalent metal phosphate-based antimicrobial particles used in the present invention are expected to have Mohs hardness of greater than 6.5. In other words, the tetravalent metal phosphate-based antimicrobial particles are expected to be harder than anatase titanium dioxide. Thus, one of ordinary skill in the art would not have been motivated to use the tetravalent metal phosphate-based antimicrobial particles of the present invention together with the inorganic compound particles such as titanium dioxide as taught by Wells with a reasonable expectation of success.

Moreover, in Wells, anatase titanium dioxide is added in order to deluster synthetic fibers (see column 3, lines 3 to 4). On the other hand, in the present invention, the inorganic particles are added in order to improve the processability of a fiber or a film to which the antimicrobial composition is added. The object of adding the inorganic particles is very different.

In Wells, in order to deluster synthetic fibers, it is preferable for anatase titanium dioxide to be fine and the preferred average diameter is 0.1 to 0.5 µm, most preferably 0.2 µm or less (see column 3, lines 15 to 16). The specific diameter of the anatase titanium dioxide used in the Example of Wells is not disclosed. That is, Wells is silent as to the average particle size of anatase titanium dioxide specifically employed in the Example.

In the present invention, if the average particle size of less than 0.1 μm, when mixed with a fiber resin they aggregate and thus easily form coarse particles, thereby causing filter blockage and filament breakage during melt spinning.

Thus, the preferred diameter of the inorganic particles in the present invention is different from that taught in the prior art due to the difference of the object of adding the inorganic particles.

Further, as admitted by the Examiner, Wells et al does not teach nor suggest the use of the tetravalent metal phosphate particle as an antimicrobial agent. Therefore, one of ordinary skill in the art would not use the tetravalent metal phosphate-based antimicrobial agent which has an average particle size being equal to or larger than the inorganic powder having a Mohs hardness of equal to or less than 6.

Even further, as previously pointed out, the present invention provides unexpectedly superior results. Comparing Example 4 and Comparative Example 4 of the present application, Comparative Example 4, which uses an inorganic compound having a larger average particle size than that of the tetravalent metal phosphate-based antimicrobial agent, causes a much greater number of filament breakages than that of Example 4 which uses an inorganic compound having an equal average particle size as that of tetravalent metal phosphate-based antimicrobial agent.

By using the inorganic compound having an average particle size equal to or less than that of the tetravalent metal-based antimicrobial agent, the number of filament breakages can be suppressed. This superior result is unpredictable and would not have been reasonably expected by those of ordinary skill based on the disclosure of Koji et al and Wells et al, whether taken alone or in combination.

Accordingly, Applicants respectfully request withdrawal of the rejection.

**B.**     **Hideki et al in view of Wells**

Claims 1, 4-6, 9-11 and 14-19 are rejected under 35 U.S.C. § 103(a) as allegedly being unpatentable over Hideki et al (JP 10-265314) in view of Wells et al.

The Examiner asserts that Hideki et al teaches an example wherein the antimicrobial powder has a mean particle diameter of 0.9 μm or 1.3 μm, and the calcium-carbonate powder has a mean particle diameter of 9.7 μm ([0017] and [0018]).

The Examiner further relies on Wells et al as teaching that titanium dioxide is a particularly preferred additive in spinning highly viscous synthetic polymer fibers used to decrease the luster of the resulting fiber spun from the molten polymer, wherein the preferred average diameter is 0.1 to 0.5 μm, most preferably 0.2 μm or less. Therefore, one of ordinary skill in the art would have been motivated to use titanium dioxide with an average diameter of approximately 0.2 μm, which would be smaller than the particles size of the tetravalent metal phosphate-based particles.

Applicants traverse the rejection and submit that the Examiner has not set forth a *prima facie* showing of obviousness. Specifically, there is no motivation for one of ordinary skill in the art to combine the references and to use the tetravalent metal phosphate-based antimicrobial particles together with the inorganic compound particles such as titanium dioxide for the reasons discussed above.

Hideki et al also fails to disclose, teach or suggest the feature of the average particle size of the inorganic compound particles is equal to or smaller than the average particle size of the tetravalent metal phosphate-based antimicrobial particles as recited in present claim 1.

Hideki et al does not describe an inorganic compound having an average particle size of 0.1 to 5 μm. Hideki et al uses CaCO₃ particles having the average particle size of 9.7 μm which does not fall within the scope of the present invention.

Furthermore, Hideki uses an inorganic compound having an average particle size that is larger than that of the tetravalent metal phosphate-based antimicrobial agent of the present invention.

The Examiner relies on Wells as teaching that titanium dioxide is a particularly preferred additive in spinning highly viscous synthetic polymer fibers used to decrease the luster resulting fiber spun from the molten polymer, wherein the preferred average diameter is 0.1 to 0.5 μm, most preferably 0.2 μm or less. Thus, the Examiner asserts that one of ordinary skill in the art would have been motivated to use the titanium dioxide with an average diameter of approximately 0.2 μm, which would have been smaller than the particle size of the tetravalent metal phosphate-based particles.

Applicants disagree.

As noted above, in column 3, lines 2 to 5, Wells describes that "Anatase titanium dioxide is the preferred form for delustering synthetic fibers because it is softer than rutile, thereby giving lower abrasiveness in yarn processing equipment". One skilled in the art would not be motivated to apply a powder material harder than anatase titanium dioxide to the dispersion for incorporation with polyamide or polyester polymer. In other word, Wells **teaches away** from particles harder than the anatase titanium dioxide for the reasons set forth above.

Therefore, one skilled in the art who considers the disclosure of Hideki et al would not use an inorganic compound having an average particle size of 0.1 to 5 μm, and would not use an inorganic compound having an average particle size equal to or smaller than that of the

tetravalent metal phosphate-based antimicrobial agent. Thus, the present invention is not rendered obvious by Hideki et al and Wells et al, whether taken alone or in combination.

Accordingly, Applicants respectfully request withdrawal of the rejection.

## II.  New Claims

New claims 20-22 ultimately depend from claim 1 and are patentable for at least the same reasons.

New claim 20 recites an average particle size of 0.2 to 2 μm, which is not disclosed, taught or suggested by Wells et al, which is relied on by the Examiner. For this additional reason, new claim 20 is patentable over the cited references, whether taken alone or in combination.

New claim 21 recites an embodiment wherein the average particle size of the tetravalent metal phosphate-based antimicrobial particles and the inorganic compound particles have an average particle size substantially in the range of 0.4 to 0.9 μm, which is not taught or suggested by Wells et al. For this additional reason, new claim 21 is patentable over the cited references, whether taken alone or in combination.

New claim 22 recites and embodiment wherein an additive ingredient can be added. In Wells, glyceride is an essential component of the dispersion for incorporation with a polyamide polymer or a polyester polymer. However, new claim 22 does not include the addition of glyceride in the resin composition. For this additional reason, new claim 22 is patentable over the cited references, whether taken alone or in combination.
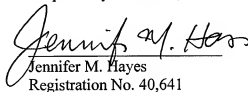
## III.  Conclusion

In view of the above, reconsideration and allowance of this application are now believed to be in order, and such actions are hereby solicited. If any points remain in issue which the

Examiner feels may be best resolved through a personal or telephone interview, the Examiner is

kindly requested to contact the undersigned at the telephone number listed below.

      The USPTO is directed and authorized to charge all required fees, except for the Issue

Fee and the Publication Fee, to Deposit Account No. 19-4880.   Please also credit any

overpayments to said Deposit Account.

                                   Respectfully submitted,

                                   *Jennifer M. Hayes*

SUGHRUE MION, PLLC                  Jennifer M. Hayes
Telephone: (202) 293-7060             Registration No. 40,641
Facsimile: (202) 293-7860

WASHINGTON OFFICE

23373

CUSTOMER NUMBER

Date: July 17, 2009

# THERMOPHYSICAL PROPERTIES OF NZP CERAMICS (A REVIEW)

## V. I. Pet'kov[1] and E. A. Asabina[1]

Data on the thermophysical properties of NZP ceramics with the $NaZr_2(PO_4)_3$-type structure are summarized. A system of thermal expansion regularities is proposed making it possible to predict NZP materials with controllable thermal expansion, including ultralow expansion with near-zero anisotropy. The thermodynamic functions of the reactions of synthesis of NZP phosphates are calculated and the applicability of ceramic technology is justified. It is proposed to use NZP ceramics as heat-insulating materials capable of working under abrupt temperature shifts.

The NZP crystallographic family with the basic structure of phosphate $NaZr_2(PO_4)_3$ includes compounds and solid solutions described by the chrystallochemical formula

$$(M1)_{0 \to 1}(M2)_{0 \to 3}\{[L_2(XO_4)_3]^{p-}\}_{3\infty},$$

where $\{[L_2(XO_4)_3]^{p-}\}_{3\infty}$ is the skeletal framework ($p$ is the charge of the skeleton); $(M1)_{0 \to 1}$, $(M2)_{0 \to 3}$ are the types of non-skeletal cation positions denoting the number of positions in each type.

The skeletal framework is formed by $LO_6$ octahedra and $XO_4$ tetrahedra joined by their vertices (Fig. 1); the vacancies M1 and M2 have different sizes and are convenient for incorporating a wide range of charge-compensating cations.

The majority of the representatives of the NZP family contain phosphor as the anion-forming element X. There are NZP-structure phases known in which phosphor is fully or partially replaced by silicon, germanium, arsenic, vanadium, sulfur, molybdenum, or tungsten. The structure-forming cations L with predominantly covalent metal – oxygen bonds have degrees of oxidation ranging from +1 to +5. These are, for instance, $Nb^{5+}$, $Ta^{5+}$, $Ti^{4+}$, $Hf^{4+}$, $Ge^{4+}$, $Sn^{4+}$, $Mo^{4+}$, $U^{4+}$, $Sc^{3+}$, $Y^{3+}$, $Ln^{3+}$ (lanthanides), $V^{3+}$, $Cr^{3+}$, $Fe^{3+}$, $Al^{3+}$, $Ga^{3+}$, $In^{3+}$, $Ti^{3+}$, $Mg^{2+}$, $Mn^{2+}$, $Cu^{2+}$, $Co^{2+}$, $Ni^{2+}$, $Zn^{2+}$, $Na^+$, and others. The positions L of the skeleton are frequently occupied by a combination of these cations. The non-skeleton positions M1 and M2 may be filled by the same or different cations, mainly low-charge ones with degree of oxidation from +1 to +4, or they may stay vacant depending on the degree of oxidation of the ions in positions L and X and the electroneutrality of the compound in general.

The resistance of an NZP structure to fluctuations in the chemical composition, temperature, and pressure is determined by relatively rigid structural fragments $L_2(XO_4)_3$ with strong bonds inside the group and uniformly distributed vacancies of different sizes, which act as buffers in the case of distortion of the skeleton as a consequence of its reaction with the non-skeletal cations. Considering the wide isomorphism (mutual substitution) of cations in all crystallographic positions (M, L, and X), the possibility of ions of different degrees of oxidization and sizes occupying the skeletal positions, and also diverse variants of the skeletal charge compensation, the set of compounds and solid solutions, either known or predicted based on crystallochemical data, becomes quite extensive. A controlled modification of the NZP phase compositions provides for ample diversity, smooth variations, and control of its properties.

The increasing interest in materials with the NZP-type structure is due to the expanding possibilities of using them as high-tech ceramics that have the unique ability of not expanding under heating. This property of phosphates along with their high melting temperatures (Table 1) and physicomechanical parameters (bending strength 1100 MPa, Young's
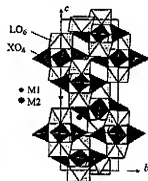


Fig. 1. Crystal structure of NZP ceramics. The skeleton consisting of L-octahedra and X-tetrahedra is indicated, as well as the nonskeleton positions M1 and M2.

[1] N. I. Lobachevskii Nizhny Novgorod State University, Nizhny Novgorod, Russia.

TABLE 1

| Compound | Melting (decomposition) temperature, K | Compound | Melting (decomposition) temperature, K |
|---|---|---|---|
| LiZr₂(PO₄)₃ | 1963 | Ba₀.₅Zr₂(PO₄)₃ | 1973 |
| NaZr₂(PO₄)₃ | 1923 | Ba₀.₅Ti₂(PO₄)₃ | 1641 |
| KZr₂(PO₄)₃ | 1883 | Ba₁₋ₓZr₄P₆₋₂ₓSi₂ₓO₂₄ | 1773 |
| Na₃Zr₂(PO₄)₃ | 1433 | Na₃Fe₂Zr₂(PO₄)₃ | 1273 |
| Mg₀.₅Zr₂(PO₄)₃ | 1273 | Ln₀.₃₃Zr₂(PO₄)₃ | 1173 |
| | | (Ln = La, Gd, Eu) | |
| Ca₀.₅Zr₂(PO₄)₃ | 1973 | Zr₃(PO₄)₄ | 1173 |
| Sr₀.₅Zr₂(PO₄)₃ | 1973 | M₀.₃₃Nb₁.₆₇(PO₄)₃ | 1173 |
| | | (M = Mg, Mn, Co, Ni) | |

$LiZr_2(PO_4)_3$ ... etc.

modulus 50 GPa, Rockwell hardness *HRA* 90, and density 3200 – 3650 kg/m³, chemical and radiation resistance, and low thermal conductivity makes them suitable for application in products that should have high resistance to thermal shock (refractory lining and its elements, fittings for high-precision soldering, semiconductor substrates, catalyst carriers, optical benches), in electronics (ceramic electrolytes, bases), in machine building and transport subsystems (engine components), and in power engineering (radiation-resistant heat-insulating materials, localizing matrices for safe storage of radioactive waste). Note that one of the common names used for the variable-composition phases $Na_{1+x}Zr_2P_{3-x}Si_xO_{12}$ with a NZP-like structure is NASICON. Other compounds having high ionic conductivity were named LISIKON, TITSICON, etc. Researchers of solid electrolytes who use these abbreviations relate samples to their composition and not to their structure. On the other hand, specialists in the sphere of ceramics dealing with materials that are structural analogs of the phosphate $NaZr_2(PO_4)_3$ prefer the name NZP, which describes the family of compounds with the same type of structure and skeleton, although the overwhelming majority of this family are not sodium-bearing compounds and not ionic conductors.

In view of the start of production of NZP ceramics [1] and expansion of its application areas, it becomes necessary to determining its general regularities relating its composition and properties. The purpose of the present study is to determine the regularities correlating the composition, structural transformations, and thermophysical properties of NZP materials, as well as the thermal resistance of ceramics and admissible fluctuations of temperatures and its gradients. These properties, such as thermal expansion, heat capacity, and thermal conductivity, have fundamental significance regardless of the application areas of these ceramics.

The most characteristic property depending on the distribution of the force of the chemical bonds in a structure is thermal expansion: the less strong the bonds between the atoms, the greater the thermal expansion. For NZP-like lattices the thermal expansion is determined by the TCLE measured parallel to $\alpha_c$ and perpendicular to $\alpha_a$, which is the

main crystal axis, and the average TCLE is $\alpha_{av} = (2\alpha_a + \alpha_c)/3$.

The majority of little-expanding materials of the NZP family [3, 4] have anisotropic thermal expansion and large absolute TCLE values and, nevertheless, low average TCLEs, for instance $NaZr_2(PO_4)_3$, (D = Zr, Hf, Ti), $RbZr_2(PO_4)_3$, $Ca_{0.5}Zr_2(PO_4)_3$, $Cd_{0.5}Zr_2(PO_4)_3$ (Table 2). This is due to the fact that the TCLE in these particular compounds along the directions determined by the crystal symmetry have opposite signs. Similarly, the best of the known little-expanding materials, such as zircon, cordierite, or quartz glass, have virtually zero expansion ($\alpha_{av} = (0.5 - 4.2) \times 10^{-6}$ K⁻¹ in the temperature interval of 273 – 1273 K). The consequence of different thermal expansion of different components in the volume of the article or in different directions in a single-phase materials is mechanical stress on the grain boundaries, sufficient for causing cracking and disturbing the continuity of articles.

At the same time, some NZP compounds have low thermal anisotropy and low TCLE values (less than $2 \times 10^{-6}$ K⁻¹). Such properties are observed in phosphates $CsZr_2(PO_4)_3$, $CsHf_2(PO_4)_3$, $Cs_{1.3}Ln_{0.2}Zr_{1.7}(PO_4)_3$ (Ln = Pr, Sm, Gd), $Sr_{0.5}Zr_2(PO_4)_3$, $Ca_{0.5-x}Sr_xZr_2(PO_4)_3$, $Sr_{0.25}Zr_{1.5}Nb_{0.5}(PO_4)_3$ (Table 2). These phosphates, due to their ultralow thermal expansion, including near-zero TCLEs and anisotropic expansion, are capable of withstanding multiple sharp fluctuations in thermal loads (thermal shocks) and are the most promising for developing thermomechanically stable materials.

Based on our studies and the results obtained by other authors, we determined a system of empirical regularities of thermal expansion in NZP materials [4], which makes it possible to extrapolate these regularities to materials of the same structural type that have not yet been studied and perform a justified selection of ceramic compositions with optimum thermal expansion parameters.

When a NZP compound, for instance, $NaZr_2(PO_4)_3$ is heated, the weakest bonds Na(MI) – O expand much more than the strong bonds Zr(L) – O and P(X) – O; the crystal undergoes anisotropic expansion: it expands along the $c$ axis and compresses along the $a$ axis. As the result, the average TCLE of NZP compounds is very low. A series of compounds $AD_2(PO_4)_3$ (D = Ti, Sn, Hf, Zr; A = Na, K) and $LiGe_2(PO_4)_3$ exhibited a negligibly small variation of the size of the polyhedra $D(L)O_6$ and $PO_4$ with increasing temperature; therefore, the skeleton $\{[L_2(PO_4)_3]^{3-}\}_{3\infty}$ of such compounds has thermal expansion approaching zero. Due to the arrangement of the less rigid (extendable) octahedra $A(MI)O_6$ in columns parallel to the $c$ axis (Fig. 1), the heating effect leads to the expansion of the structure in the direction $c$ ($\alpha_c > 0$). In this case we observe a correlated rotation of the $LO_6$ octahedra and phosphor tetrahedra connected by their vertexes, and the structure compresses in the direction $a$ ($\alpha_a < 0$).

A correlation of the effects of heating and crystallochemical substitution on the geometrical parameters of the

crystal lattice shows that with increasing temperature an octahedron, for instance $Na(M1)O_6$, expands but not enough for sodium to be replaced by a larger alkaline metal cation and obtain the polyhedron $A(M1)O_6$ that is equivalent in size ($A = K$, Rb, or Cs). Therefore, the crystallo-chemical substitution effect and the thermal expansion effects have similar features: they are not equivalent, although they affect the same atomic bonds in the structure.

Knowing the effect of the occupied and vacant cation positions on the thermal expansion of a structure, one can predict the thermal expansion characteristics of NZP materials. The experimental data accumulated suggest that M1 positions have a deciding effect on TCLE modification.

In the case of compounds described by the general formula $AD_2(PO_4)_3$, the positions M1 are completely filled by cations $A^+$ and the positions M2 are vacant. If an occupied octahedron $AO_6$ is already extended along the crystallographic $c$ axis at room temperature due to the introduction of a larger cation, the further expansion of the structure along the $c$ axis in heating will be suppressed by the bridge $PO_4$ tetrahedra that will connect the skeletal framework columns. For instance, the axial coefficients in the phosphates series $AD_2(PO_4)_3$ ($A = Na$, K, Rb, Cs; $D = Zr$, Hf) in the temperature range from 293 to 1073 K are within the limits : $\alpha_a = (-8 \text{ to } -0.56) \times 10^{-6} \text{ K}^{-1}$, $\alpha_c = (22.3 - 0.45) \times 10^{-6} \text{ K}^{-1}$ passing from the composition with Na (ionic radius $r_{Na^+} = 1.02$ Å) to the composition with Cs ($r_{Cs^+} = 1.67$ Å). TCLEs approaching zero and nearly zero anisotropy of the axial expansion are reached in the compounds $CsD_2(PO_4)_3$ ($D = Zr$, Hf) (Table 2). Here a general tendency is observed: the larger cation filling the non-skeletal position M1 decreases both thermal expansion and the anisotropy of thermal expansion. The expansion—compression effects are the lowest in compounds with the smallest structure-forming cations $D$ of the skeleton and grow as the size of the cation $D$ increases. This relationship is determined by the fact that the more polarized metal ion to a greater extent localizes electron density on the bonds $P - O - (D)$ and the double rotation of the $PO_4$ tetrahedron and $DO_6$ octahedron under a change of temperature becomes less facile.

The presence of a 3D canal lattice in the NZP structure enables the migration of $Li^+$ and $Na^+$ cation from fully occupied M1 positions to vacant M2 positions as the temperature increases. This process is accompanied by more intense repulsion between the oxygen ion chains around the vacant M1 positions, which increases $\alpha_c$. Thus, for $LiTi_2(PO_4)_3$ the disordering of lithium cations with respect to positions M1 and

M2 under heating leads to the maximum TCLE along the $c$ axis ($\alpha_c = 30.8 \times 10^{-6} \text{ K}^{-1}$) of all the NZP materials.

If the filling of positions M1 is lower than unity and the positions M2 are vacant, which occurs, for instance, in compounds of the type $B_{0.5}D_2(PO_4)_3$ ($B = Ca$, Sr, Cd; Ba; $D = Ti$, Zr) or $Ln_{0.33}D_2(PO_4)_3$, it is necessary to take into account the contribution of the cation-filled and vacant M1 positions to the relative expansion – compression of the structure with increasing temperature. It has been noted that the filling of M1 positions expands the structure along the $c$ axis and compresses it along the $a$ axis. At the same time, vacant M1 positions can either expand or compress in heating. In this case the electrostatic mutual attraction of the cation in the position M1 and the oxygen ion disappears, and the size of the vacant M1 position is controlled by the $O - O$ distance depending on the value and the charge of the cations in the filled M1 position and in the skeletal framework. Thus, in the structures $Cd_{0.5}Zr_2(PO_4)_3$ and $Ca_{0.5}Zr_2(PO_4)_3$ the vacant positions M1 expand with increasing temperature and in $Sr_{0.5}Ti_2(PO_4)_3$ they become compressed. By combining NZP compounds
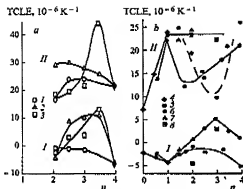
TABLE 2

| Compound | TCLE, $10^{-6}$ K$^{-1}$ | | | Anisotropy $\|\alpha_a - \alpha_c\|$, $10^{-6}$ K$^{-1}$ | Degree of anisotropy $\dfrac{\|\alpha_a - \alpha_c\|}{\|\alpha_{av}\|}$ | Published source |
|---|---|---|---|---|---|---|
| | $\alpha_a$ | $\alpha_c$ | $\alpha_{av}$ | | | |
| $NaZr_2(PO_4)_3$ | -5.50 | 22.30 | 3.80 | 27.80 | 7.30 | [5] |
| $KZr_2(PO_4)_3$ | -5.30 | 5.41 | -1.73 | 10.70 | 6.20 | [5] |
| $RbZr_2(PO_4)_3$ | -8.00 | 13.00 | -1.00 | 21.00 | 21.00 | [6] |
| $CsZr_2(PO_4)_3$ | -0.56 | 0.45 | -0.22 | 1.00 | 4.50 | [6] |
| $NaHf_2(PO_4)_3$ | -6.55 | 21.00 | 2.63 | 27.50 | 10.50 | [6] |
| $CsHf_2(PO_4)_3$ | -1.10 | 1.00 | -0.40 | 2.10 | 5.30 | [6] |
| $LiTi_2(PO_4)_3$ | 0.49 | 30.80 | 10.60 | 30.30 | 2.90 | [7] |
| $NaTi_2(PO_4)_3$ | -5.30 | 20.80 | 3.40 | 26.10 | 7.70 | [7] |
| $KTi_2(PO_4)_3$ | -0.13 | 6.62 | 2.12 | 6.70 | 3.20 | [7] |
| $Ca_{0.5}Zr_2(PO_4)_3$ | -2.57 | 7.74 | 0.87 | 10.30 | 11.80 | [9] |
| $Sr_{0.5}Zr_2(PO_4)_3$ | 2.24 | 2.28 | 2.25 | 0.00 | 0.00 | [9] |
| $Cd_{0.5}Zr_2(PO_4)_3$ | -3.50 | 10.20 | 1.10 | 13.70 | 12.50 | [5] |
| $Ba_{0.5}Zr_2(PO_4)_3$ | 5.40 | -1.80 | 3.00 | 7.20 | 2.40 | [10] |
| $Ba_{1.375}Zr_4P_{5.25}Si_{0.75}O_{24}$ | 0.14 | 0.46 | 0.25 | 0.32 | 1.28 | [2] |
| $Sr_{0.5}Hf_2(PO_4)_3$ | 1.66 | 1.67 | 1.66 | 0.00 | 0.00 | [9] |
| $Ca_{0.5}Ti_2(PO_4)_3$ | 6.99 | 1.31 | 5.10 | 5.70 | 1.10 | [9] |
| $Sr_{0.5}Ti_2(PO_4)_3$ | 9.88 | -0.14 | 6.54 | 10.00 | 1.50 | [9] |
| $Ca_{0.25}Sr_{0.25}Zr_2(PO_4)_3$ | -0.70 | 1.10 | -0.10 | 1.80 | 18.00 | [11] |
| $Sr_{0.25}Zr_{1.5}Nb_{0.5}(PO_4)_3$ | -1.30 | 2.60 | 0.00 | 3.90 | – | [12] |
| $Na_3CdZr(PO_4)_3$ | 7.04 | 13.90 | 9.30 | 6.90 | 0.70 | [5] |
| $Cs_{1.3}Pr_{0.3}Zr_{1.7}(PO_4)_3$ | -1.50 | 0.50 | -0.80 | 2.00 | 2.50 | [6] |
| $Cs_{1.3}Sm_{0.3}Zr_{1.7}(PO_4)_3$ | -0.90 | 1.30 | -0.20 | 2.10 | 10.50 | [6] |
| $Cs_{1.3}Gd_{0.3}Zr_{1.7}(PO_4)_3$ | -0.52 | -0.46 | -0.50 | 0.10 | 0.20 | [6] |
| $NbZr(PO_4)_3$ | -3.40 | 1.20 | -1.90 | 4.60 | 2.40 | [13] |
| $Mg_{0.33}Nb_{1.67}(PO_4)_3$ | -2.30 | 3.40 | -0.39 | 5.70 | 14.60 | [14] |
| $Co_{0.33}Nb_{1.67}(PO_4)_3$ | -1.50 | 4.40 | 0.47 | 5.90 | 12.60 | [14] |
| $Ni_{0.33}Nb_{1.67}(PO_4)_3$ | -2.20 | 3.00 | -0.47 | 5.20 | 11.10 | [14] |
| $Al_{0.5}Nb_{1.5}(PO_4)_3$ | -1.10 | ~0 | -0.73 | 1.10 | 1.50 | [15] |
| $Fe_{0.5}Nb_{1.5}(PO_4)_3$ | -2.60 | 1.30 | -1.30 | 3.90 | 3.00 | [15] |

Fig. 2. Dependence of TCLE $\alpha_a$ (I) and $\alpha_c$ (II) on the degree of filling M-positions in phosphates: $a$) $Na_{5-2x}B_xZr(PO_4)_3$, where $B \approx Mg$ (I), Ca (2), Sr (3); $b$) $Na_{1-x}Nb_xZr_{2-x}(PO_4)_3$ (4), $Na_3Zr_{2.25-0.25x}(PO_4)_3$ (5), $Na_{1+x}Zr_2(P_{3-x}Si_x)O_{12}$ (6), $Na_{1+x}Y_xZr_{2-x}(PO_4)_3$ (7), $Na_{1+2x}Mg_xZr_{2-x}(PO_4)_3$ (8).

with TCLEs that are close in values and opposite in signs and can form wide ranges of solid solutions, it is possible to design ceramic compositions with a controllable TCLE, including an extralow TCLE with minimal anisotropy and, accordingly, resistant to microcracking under sharp temperature fluctuations. For instance, ceramic materials based on the compounds $Ca_{0.5-x}Sr_xZr_2(PO_4)_3$ and $K_{2x}Sr_{0.5-x}Zr_2(PO_4)_3$ have minimal anisotropy close to zero [11, 16]. This is due to the fact that $KZr_2(PO_4)_3$ and $Ca_{0.5}Zr_2(PO_4)_3$ have positive TCLEs along the $c$ axis ($\alpha_c > 0$) and negative values along the $a$ axis ($\alpha_a < 0$), whereas $Sr_{0.5}Zr_2(PO_4)_3$ has positive TCLE with $\alpha_c > \alpha_a$. Consequently, intermediate compositions with close to zero expansion anisotropy may exist between the end members of the solid solution series. The results of the research established that ceramic materials of the compositions $K_{0.5}Sr_{0.4}Zr_2(PO_4)_3$ ($\alpha_{av} = 3.1 \times 10^{-6} K^{-1}$, $|\alpha_a - \alpha_c| = 0.95 \times 10^{-6} K^{-1}$) and $Ca_{0.25}Sr_{0.25}Zr_2(PO_4)_3$ ($\alpha_{av} = -0.1 \times 10^{-6} K^{-1}$, $|\alpha_a - \alpha_c| = 1.8 \times 10^{-6} K^{-1}$) have minimal thermal anisotropy.

If the positions M1 and M2 are not filled (with the skeletal charge $p = 0$), the rotations of the polyhedra are less intense and the intensity of the thermal expansion of the lattice of the "empty" skeletal changes as the ionic radius of the atom in the L position changes. Under thermal loading the expansion – compression of the lattice along the $c$ axis due to the presence of vacancies in the direction $c$ depends on the strength of the O – O and L – O bonds. The average TCLE $\alpha_{av}$ of the empty skeletons changes from $-1 \times 10^{-6}$ to $1 \times 10^{-6} K^{-1}$.

The crystallochemical nature of thermal deformations is more complex when the positions M1 are vacant and M2 are filled with cations. Thus, most phosphates $Na_3R_2(PO_4)_3$ ($R = Sc, Ti, V, Cr, Fe, Y, In, Yb$) undergo reversible phase transformations consisting in the adaptation of the structure to the changing exterior conditions (temperature, or specifies

of the synthesis of samples). The existence of polymorphism in the compounds $A_3R_2(PO_4)_3$ ($A = Li, Na$) restricts the possibility of their application as high-strength and crack-resistant materials. The data on the thermal expansion of compounds with totally filled M2 positions and vacant M1 positions are limited to a few sodium-bearing phosphates. The ceramics based on these phosphates are highly-expanding materials ($\alpha_{av} > (6-8) \times 10^{-6} K^{-1}$), since the average TCLE value of the oxygen polyhedra containing Na is high.

Substitution with filling space $Zr^{4+} \rightarrow Na^+ + R^{3+}$ in the crystal structure $NaZr_2(PO_4)_3$ leads to the formation of solid solutions $Na_{1+x}R_xZr_{2-x}(PO_4)_3$, in which cations partly fill M1 and M2 positions. Three effects are observed in such substitutions with filling space: an increasing filling of M2 positions, which causes the skeleton to expand along the $a$ axis and compressing along the $c$ axis; a change in the number of vacancies in M1 positions leading to the expansion – compression of the M1 positions (vacancies); a very insignificant skeletal expansion due to the replacement of some $Zr^{4+}$ cations by larger cations. The dependences of the TCLE ($\alpha_a$ and $\alpha_c$) on the degree of filling of the M-positions in the compounds and solid solutions investigated by us [5, 17] or described in the literature [13]: $Na_{5-4x}Zr_xZr(PO_4)_3$, $Na_{5-2x}B_xZr(PO_4)_3$ (B = Mg, Cu, Sr), $Na_{5-2x}Fe_xZr(PO_4)_3$, $Na_{1-x}Nb_xZr_{2-x}(PO_4)_3$,     $Na_{1+x}Zr_2(P_{3-x}Si_x)O_{12}$, $Na_{1+x}Y_xZr_{2-x}(PO_4)_3$, and $Na_{1+2x}Mg_xZr_{2-x}(PO_4)_3$ are complex and nonmonotonic.

With increasing degree of filling of the M-positions, the TCLE along the $a$ axis ($\alpha_a$) is usually negative (Fig. 2); sometimes it grows and transforms from a negative into a positive one, whereas $\alpha_c$ remains large ($\alpha_c > 0$). This tendency persists up to the filling M-positions equal to $1 - 2.5$. The axial anisotropy in this case is determined. As the filling of M-positions grows from $2 - 2.5$ to 3.5, the TCLEs for both directions may be positive, whereas $\alpha_c$ usually decreases and the anisotropy increases again. This change in the TCLE may be explained as follows. Under a certain degree of filling of the positions M1 and M2, the thermal expansion effect along the $a$ axis becomes comparable to the expansion effect along the $c$ axis, and later on expansion along the $c$ axis may become the predominant one.

With full occupancy of M1 and M2 positions by cations, for instance in the phosphate $Na_3Zr(PO_4)_3$, the deciding effect in thermal expansion parameters is exerted by the size of the cation in the M-positions and the average thermal expansion of the metal ($M^+$) – oxygen bond. One can expect a decrease in the absolute values of $\alpha_a$ and $\alpha_c$ and a decrease in anisotropy as the size of the cations filling all M-positions grows.
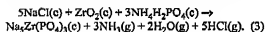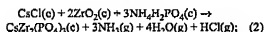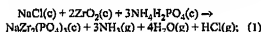
The above regularities of thermal expansion of NZP-type compounds provide a scientific interpretation of the processes of formation of materials with required properties, i.e., makes it possible to deliberately design new ceramic materials with controlled TCLE, including a low TCLE with near-zero anisotropy.

The precision determination of the heat capacity that characterizes the quantity of thermal energy required for a certain change in the temperature of the material and thermal conductivity that characterizes the quantity of heat transmitted through the material under a preset temperature gradient are labor-consuming operations. That is why data on heat capacity and thermal conductivity are limited to a few representatives of the NZP family.

The heat capacity of different materials in the NZP family is $0.5-1.0$ J/(g·K) in the temperature interval of $273-623$ K (Fig. 3). An important property of specific heat is that it is independence of the microstructure of the material (apparent density, porosity, distribution of pores by shape and size) at high temperatures. The heat capacity of most materials investigated grows monotonically with increasing temperature and change insignificantly in the temperature above 500 K. The heat capacity curves of $Na_5Zr(PO_4)_3$, $Na_3Fe_2(PO_4)_3$, and $Na_3Cr_2(PO_4)_3$ exhibit anomalies (phase transformations) related either to a modification of the position ordering of sodium cations in the skeletal vacancies of the first compound (transformation temperature 406.9 K) or to the processes of antiferromagnetic ordering for the two latter compounds (at temperatures of 47 and 12 K, respectively).

Data on heat capacity and other thermodynamic functions are needed to study the thermodynamic aspect of synthesis and stability of NZP materials. The use of thermodynamic methods makes it possible to learn which of the possible chemical reactions may occur spontaneously at the preset conditions (temperature, pressure, concentration) and how the conditions should be modified for the specified process to proceed in a required direction with a sufficient product yield.

The initial materials in solid-phase synthesis of NZP ceramics are usually alkali metal salts, zirconium oxide, and ammonium dihydrophosphate (the chemical formulas of the compounds are followed by a letter in brackets indicating their physical state: "c" for crystal and "g" for gas):

$$NaCl(c) + 2ZrO_2(c) + 3NH_4H_2PO_4(c) \rightarrow$$
$$NaZr_2(PO_4)_3(c) + 3NH_3(g) + 4H_2O(g) + HCl(g); \quad (1)$$

$$CsCl(c) + 2ZrO_2(c) + 3NH_4H_2PO_4(c) \rightarrow$$
$$CsZr_2(PO_4)_3(c) + 3NH_3(g) + 4H_2O(g) + HCl(g); \quad (2)$$

$$5NaCl(c) + ZrO_2(c) + 3NH_4H_2PO_4(c) \rightarrow$$
$$Na_5Zr(PO_4)_3(c) + 3NH_3(g) + 2H_2O(g) + 5HCl(g). \quad (3)$$

To analyze the conditions of the formation of NZP products, standard thermodynamic functions for their formation of synthesis have been calculated (Table 3). The enthalpy (thermal effects) of the reactions considered $\Delta_r H^0(298)$ at a temperature of 298.15 K were calculated in accordance with the Hess law based on the standard formation enthalpy at the same temperature $\Delta_f H^0(298)$ of the respec-
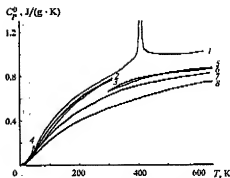


Fig. 3. Temperature dependences of heat capacity $C_p^0$ of crystalline compounds: $Na_5Zr(PO_4)_3$ (1), $Na_3Cr_2(PO_4)_3$ (2), $Na_3MgZr(PO_4)_3$ (3), $Na_4Fe_2(PO_4)_3$ (4), $Na_4Zr_2Si_3O_{12}$ (5), $Na_5Zr_2Si_2O_{12}$ (6), $NaZr_2(PO_4)_3$ (7) and $CsZr_2(PO_4)_3$ (8).

tive reactants. The entropy (the measures of irreversible energy dissipation) of the reactions $\Delta_r S^0(298)$ were calculated based on the values of the absolute entropy of the reactants at the temperature specified. The standard thermodynamic functions $\Delta_r H^0(T)$ and $\Delta_r S^0(T)$ at temperatures $T$ above 298.15 K were calculated based on general thermodynamic relations provided that the algebraic sum of the heat capacities of the reactants taking into account their stoichiometric coefficients $\Delta(n\,C_p^0)$ at 298.15 K is constant in the temperature interval from 298.15 K to $T$:

$$\Delta_r H^0(T) = \Delta_r H^0(298) + \Delta(n\,C_p^0)(T - 298.15);$$

$$\Delta_r S^0(T) = \Delta_r S^0(298) + \Delta(n\,C_p^0)\ln(T/298.15).$$

The standard Gibbs function of the reactions at all temperatures was calculated from the equation

$$\Delta_r G^0(T) = \Delta_r H^0(T) - T\Delta_r S^0(T).$$

If $\Delta_r G^0 < 0$, the reaction tends to be spontaneous in the direction "reactants → products."

TABLE 3

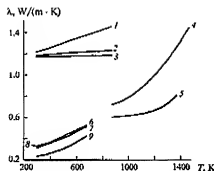| Compound | $C_p^0$(298), J/(g·K) | $-\Delta_f H^0$(298), kJ/g | $-\Delta_f S^0$(298), J/(g·K) | $-\Delta_f G^0$(298), kJ/g | Published source |
|---|---|---|---|---|---|
| $NaZr_2(PO_4)_3$ | 0.6238 | 10.67 | 2.25 | 10.00 | [18] |
| $KZr_2(PO_4)_3$ | – | 10.43 | – | – | [19] |
| $RbZr_2(PO_4)_3$ | – | 9.59 | – | – | [19] |
| $CsZr_2(PO_4)_3$ | 0.5122 | 8.83 | 1.88 | 8.27 | [19] |
| $Na_5Zr(PO_4)_3$ | 0.7919 | 11.37 | 2.36 | 10.67 | [20] |
| $Na_3Fe_2(PO_4)_3$ | 0.7586 | – | 2.51 | – | [21] |
| $Na_3Cr_2(PO_4)_3$ | 0.7570 | – | 2.62 | – | [21] |
| $Na_3MgZr(PO_4)_3$ | 0.7473 | – | 2.55 | – | [21] |
| $Na_5Zr_2Si_3O_{12}$ | 0.6623 | 10.96 | 2.09 | 10.34 | [22] |
| $Na_4Zr_2Si_3O_{12}$ | 0.6632 | 11.41 | 2.08 | 10.79 | [22] |

Fig. 4. Temperature dependences of thermal conductivity $\lambda$ of high-density ($1-5$) and low-density ($6-9$) types of NZP ceramics: $Ca_{0.5}Mg_{0.5}Zr_2(PO_4)_6$ ($1$), $Cu_{0.5}Zr_{4.06}(PO_4)_6$ ($2$), $Ca_{0.5}Zr_2(PO_4)_6$ ($3$), $Ca_{0.5}Mg_{0.5}Zr_2(PO_4)_6$ ($4$), $Ca_{0.5}Mg_{0.5}Zr_2(PO_4)_6$ ($5$), $Zr_3(PO_4)_4$ ($6$), $CSZr_2(PO_4)_3$ ($7$), $NaZr_2(PO_4)_3$ ($8$), and $Na_4Zr(PO_4)_3$ ($9$).

It can be seen from the data in Table 4 that the reactions used for the synthesis of NZP materials are endothermic. The Gibbs functions at 298.15 K of the reactions of synthesis are positive, i.e., the equilibrium at the temperatures specified is shifted toward the initial materials. The synthesis temperatures above which the processes (1) – (3) are thermodynamically resolved at a standard pressure are not high and amount to approximately 430 K for $NaZr_2(PO_4)_3$, about 410 K for $CSZr_2(PO_4)_3$, and about 570 K for $Na_4Zr(PO_4)_3$. For this reason, ceramic technology is a common method for producing NZP materials.

To predict application areas for NZP ceramics and improve their production technologies, one has to know the rate of temperature change in the article under heat treatment or during service, i.e., its thermal conductivity and heat capacity. The thermal conductivity of ceramics depends both on its crystal structure (the more complicated is the crystal lattice and the more defective its structure, the lower is the thermal conductivity) and its ceramic structure (organization of crystallites of the same or different compositions in the volume of polycrystalline bodies). The temperature dependences of the thermal conductivity of known high-density (porosity below 10%) and low-density (porosity 26 – 38%) kinds of NZP ceramics are shown in Fig. 4. It can be seen that the dependences within the temperature interval considered have no peculiarities and the thermal conductivity grows smoothly

with increasing temperature. The dependence of the thermal conductivity of NZP ceramics on its porosity is obvious in the physical context. As the thermal conductivity of low-density ceramics is an intermediate value between the thermal conductivity of the main material and the thermal conductivity of air contained in the pores between the particles, it is evident that due to the large difference between the thermal conductivity of the solid and gaseous phases, the looser ceramic with a higher content of air and with intense disturbance of intergrain contacts will have the lower thermal conductivity. For low-density materials the thermal conductivity with zero porosity can be calculated from the formula [23]

$$\lambda = \lambda_0 \frac{1 + 2V_p(1 - \lambda_0/\lambda_a)(2\lambda_0/\lambda_a + 1)^{-1}}{1 - V_p(1 - \lambda_0/\lambda_a)(\lambda_0/\lambda_a + 1)^{-1}},$$

where $\lambda$, $\lambda_0$, and $\lambda_a$ are the thermal conductivities of the porous body, its solid phase, and the gas (air) in its pores, respectively; $V_p$ is the volume fraction of pores in the porous body.

The calculated thermal conductivity values with zero porosity within the temperature interval of 298 – 673 K are equal to (W/(m·K)): 0.6 – 1.1 for $Zr_3(PO_4)_3$, 0.6 – 0.9 for $NaZr_2(PO_4)_3$, 0.7 – 1.1 for $CSZr_2(PO_4)_3$ and 0.4 – 0.7 for $Na_4Zr(PO_4)_3$ [24]. These values satisfactorily agree with the data on the thermal conductivity of high-density NZP ceramics ($\lambda = 0.6 - 1.4$ W/(m·K), $298 < T < 873$ K) [25] (U.S. patent No. 5102836). Thermal conductivity in thermal calculations is usually taken as the mean working temperature of a particular product (material).

It is notable that despite the spread in thermal conductivity values found in the literature caused by the chemical and phase compositions of the tested NZP materials, specifics of their crystal structure (valence of ions, their distribution in the crystal lattice, type and number of defects, the type of chemical bond), microstructural organization (size, dispersion, shape of grains, and porosity type), as well as specifics of measuring methods, NZP ceramics has lower thermal conductivity than stabilized zirconium dioxide (1.95 – 2.44 W/(m·K) in the temperature interval of 373 – 1673 K), which is the main component in widely used refractories for heat-enclosing structures of high-temperature furnaces. Ultralow thermal conductivity, high melting temperatures, ultralow thermal expansion with nearly zero aniso-

TABLE 4

| $T$, K | $\Delta_r H^0$, kJ/g, for reaction | | | $\Delta_r S^0$, J/(g·K), for reaction | | | $\Delta_r G^0$, kJ/g, for reaction | | |
|---|---|---|---|---|---|---|---|---|---|
| | (1) | (2) | (3) | (1) | (2) | (3) | (1) | (2) | (3) |
| 298.15 | 1.061 | 0.802 | 1.679 | 2.484 | 1.990 | 2.964 | 0.320 | 0.208 | 0.796 |
| 400 | 1.058 | 0.799 | 1.674 | 2.476 | 1.983 | 2.947 | 0.068 | 0.006 | 0.495 |
| 450 | 1.057 | 0.798 | 1.671 | 2.474 | 1.980 | 2.941 | −0.007 | −0.093 | 0.347 |
| 500 | 1.055 | 0.797 | 1.668 | 2.469 | 1.978 | 2.935 | −0.180 | −0.192 | 0.201 |
| 550 | 1.054 | 0.796 | 1.665 | 2.467 | 1.976 | 2.930 | −0.303 | −0.291 | 0.054 |
| 600 | 1.052 | 0.794 | 1.663 | 2.464 | 1.974 | 2.925 | −0.426 | −0.390 | −0.092 |

tropy, and chemical and radiation resistance suggest that NZP ceramics are promising heat-insulating materials exceeding the known high-temperature insulators [23] in their capacity to withstand thermal shocks.

Considering the growing interest in the industrial production of NZP ceramics that have a unique set of physical and physicochemical properties fortunately combined in the same material and using the results of analysis of its thermophysical properties, taking into account crystallochemical data and chemical compositions will make it possible to develop new types of ceramics capable of resisting thermal shocks and possessing the required level of thermophysical parameters.

## REFERENCES

1. "NZP ceramics, a new class of materials," *Am. Ceram. Soc. Bull.*, 76(10), 71 – 72 (1997).
2. S. I. Novikova, *Thermal Expansion of Solids* [in Russian], Nauka, Moscow (1974).
3. E. Breval and D. K. Agrawal, "Thermal expansion characteristics of NZP, NaZr$_2$(PO$_4$)$_3$-type materials: a review," *Br. Ceram. Trans.*, 94(1), 27 – 32 (1995).
4. V. I. Pet'kov and A. I. Orlova, "Crystallochemical approach to predicting thermal expansion of compounds with the sodium-dizirconium phosphate structure," *Neorg. Mater.*, 39(10), 1177 – 1188 (2003).
5. V. I. Pet'kov, A. I. Orlova, G. N. Kazantsev, et al., "Thermal expansion in the Zr- and 1-, 2-valent complex phosphates of NaZr$_2$(PO$_4$)$_3$ (NZP) structure," *J. Therm. Anal. Calorim.*, 66(2), 623 – 632 (2001).
6. A. I. Orlova, G. N. Kazantsev, and S. G. Samoilov, "Ultralow thermal expansion in the Cs – Ln – Zr and M – Hf phosphates (Ln = Pr, Sm, Gd; M = Na, K, Rb, Cs)," *High Temp. – High Press.*, 31(1), 105 – 111 (1999).
7. D. A. Woodcock and P. Lightfoot, "Comparison of the structural behavior of the low-thermal expansion NZP phases MTi$_2$(PO$_4$)$_3$ (M = Li, Na, K)," *J. Mater. Chem.*, 9(11), 2907 – 2911 (1999).
8. R. Brochu, M. Lour, M. Alami et al., "Structure and thermal expansion of KGe$_2$(PO$_4$)$_3$," *Mater. Res. Bull.*, 32(1), 113 – 122 (1997).
9. K. V. Govindan Kutty, R. Asuvathraman, and R. Sridharan, "Thermal expansion studies on the sodium zirconium phosphate family of compounds A$_{1/2}$M$_2$(PO$_4$)$_3$: effect of interstitial and framework cations," *J. Mater. Sci.*, 33(15), 4007 – 4013 (1998).
10. S. Y. Limaye, D. K. Agrawal, and H. A. McKinstry, "Synthesis and thermal expansion of MZr$_4$P$_6$O$_{24}$ (M = Mg, Ca, Sr, Ba)," *J. Am. Ceram. Soc.*, 70(10), C232 – C236 (1987).
11. S. Y. Limaye, D. K. Agrawal, R. Roy, and Y. Mehrotra, "Synthesis, sintering and thermal expansion of Ca$_{1-x}$Sr$_x$Zr$_4$P$_6$O$_{24}$, an ultralow thermal expansion ceramic system," *J. Mater. Sci.*, 26(1), 93 – 98 (1991).
12. T. Ota, P. Jin, and I. Yamai, "Low thermal expansion and low thermal expansion anisotropy ceramic of Sr$_{0.5}$Zr$_2$(PO$_4$)$_3$ system," *J. Mater. Sci.*, 24, 4239 – 4245 (1989).
13. T. Ota and I. Yamai, "Low thermal expansion behavior of NaZr$_2$(PO$_4$)$_3$-type compounds," *J. Am. Ceram. Soc.*, 69(1), 1 – 6 (1986).
14. A. I. Orlova, V. I. Pet'kov, M. V. Zharinova, et al., "Synthesis and thermal expansion of complex niobium (V) phosphates with bivalent elements," *Zh. Prikl. Khim.*, 76(1), 14 – 17 (2003).
15. M. V. Zharinova, A. I. Orlova, A. K. Koryttseva, et al., "New niobium phosphates. Synthesis, crystallochemical studies, behavior in heating," *Zh. Prikl. Khim.*, 49(2), 174 – 180 (2004).
16. D.-M. Liu, L.-J. Lin, and C.-J. Chem, "Thermal expansion and crystal chemistry of (Sr$_{1-x}$K$_{2x}$)Zr$_4$(PO$_4$)$_6$ ceramic," *J. Appl. Crystallogr.*, 28, 508 – 512 (1995).
17. A. I. Orlova, D. V. Kemenov, V. I. Pet'kov, et al., "Ultralow and negative thermal expansion in zirconium phosphate ceramics," *High Temp. – High Press.*, 34(3), 315 – 322 (2002).
18. V. I. Pet'kov, K. V. Kir'yanov, A. I. Orlova, and D. B. Kitaev, "Thermodynamic properties of the phosphate NaZr$_2$(PO$_4$)$_3$," *Neorg. Mater.*, 36(4), 478 – 483 (2000).
19. V. I. Pet'kov, K. V. Kyr'anov, A. I. Orlova, and D. B. Kitaev, "Thermodynamic properties of the MZr$_2$(PO$_4$)$_3$ (M = Na, K, Rb or Cs) compounds," *J. Therm. Anal. Calorim.*, 65(2), 381 – 389 (2001).
20. V. I. Pet'kov, K. V. Kir'yanov and E. A. Asabina, "Thermodynamic properties of crystalline pentasodium zirconium tris(phosphate)," *Zh. Fiz. Khim.*, 77(5), 797 – 802 (2003).
21. L. Abello, K. Chhor, M. Barj, et al., "Heat capacity and Na$^+$ ion disorder in NASICON-type solid electrolytes Na$_3$M$_2$P$_3$O$_{12}$ (M$_2$ = Fe$_2$, Cr$_2$, ZrMg) in the temperature range 10 to 300 K," *J. Mater. Sci.*, 24(9), 3380 – 3386 (1989).
22. U. Warhus, J. Maier, and A. Rabenau, "Thermodynamics of NASICON (Na$_{1+x}$Zr$_2$Si$_x$P$_{3-x}$O$_{12}$)," *J. Solid State Chem.*, 72(1), 113 – 125 (1988).
23. W. J. Kingery, *Introduction to Ceramics* [Russian translation], Stroiizdat, Moscow (1967).
24. V. I. Pet'kov, V. N. Loshkarev, and E. A. Asabina, "Thermal conductivity of zirconium phosphates and alkali metals (Na, Cs) of the family NaZr$_2$(PO$_4$)$_3$," *Zh. Prikl. Khim.*, 77(2), 184 – 187 (2004).
25. D.-M. Liu, "Thermal conduction behaviour of (Ca, X)Zr$_4$(PO$_4$)$_6$ ceramic (X = Li, Mg, Zr)," *J. Mater. Sci. Lett.*, 13(2), 129 – 130 (1994).

# CiDRA®Precision Services, LLC

## Making the Impossible Routine℠...

## Mineral Hardness Conversion Chart

There are many different scales / methods to measure mineral hardness. The most appropriate method for your application will depend on the material that you are measuring. The chart below is intended to give you a general reference of how some of these methods relate to others, using Mohs as the base measurement.

### Hardness Comparison Reference Chart

| Mohs (MH) | Knoop (HK) | Brinell Indentation (HB Indentation) | Brinell 10mm Standard 500 kgf (HB 500) | Rockwell A-Scale (HRA) | Vickers (HV) | Material Example |
|---|---|---|---|---|---|---|
| 1 | -- | -- | -- | -- | 27 | Talc |
| 2 | -- | -- | -- | -- | 61 | Gypsum |
| 2.5 | 117 | -- | 90 | -- | 102 | -- |
| 3 | 169 | 4.9 | 136 | -- | 157 | Calcite |
| 3.5 | 239 | 4.10 | 189 | 60 | 229 | -- |
| 4 | 327 | 3.50 | -- | 66 | 315 | Fluorite |
| 4.5 | 436 | 3.08 | -- | 72 | 418 | -- |
| 5 | 564 | 2.76 | -- | 77 | 535 | Apatite |
| 5.5 | 705 | 2.44 | -- | 81 | 669 | -- |
| 6 | 839 | 2.27 | -- | 84 | 817 | Feldspar |
| 6.5 | 929 | -- | -- | 85 | 982 | -- |
| 7 | -- | -- | -- | -- | 1151 | Quartz |
| 8 | -- | -- | -- | -- | 1567 | Topaz |
| 9 | -- | -- | -- | -- | 2035 | Corundum |
| 10 | -- | -- | -- | -- | -- | Diamond |

"--" = converted value is outside of acceptable range for this scale.